Kuwait J. Sci. **48 (1)** pp. 14-24, 2021

Two efficient numerical methods for solving Rosenau-KdV-RLW equation

Sibel Özer*

Dept. of Mathematics, Inonu University,

Malatya, Turkey

**Corresponding author: sibel.ozer@inonu.edu.tr*

Abstract

In this study, two efficient numerical schemes based on B-spline finite element method (FEM) and time-splitting methods for solving Rosenau-KdV-RLW equation are presented. In the first method, the equation is solved by cubic B-spline Galerkin FEM. For the second method, after splitting Rosenau-KdV-RLW equation in time, it is solved by Strang time-splitting technique using cubic B-spline Galerkin FEM. The differential equation system in the methods is solved by the fourth-order Runge-Kutta method. The stability analysis of the methods is performed. Both methods are applied to an example. The obtained numerical results are compared with some methods available in the literature via the error norms L_2 and L_∞, convergence rates, and mass and energy conservation constants. The present results are found to be consistent with the compared ones.

Keywords: Cubic B-spline functions; Galerkin method; Rosenau-KdV-RLW; Strang time-splitting.

1. Introduction

High-order nonlinear evolution equations have a special place in PDEs. Rosenau-type high-order nonlinear evolution equations are of the form

$$U_t + U_{xxxxt} = -F(U, U_x, U_{xx}, U_{xxx}, U_{xxt}), \quad (x,t) \in \Omega \times [0,T] \tag{1}$$

with the initial condition

$$U(x,0) = U_0(x), \, x \in \Omega$$

and the boundary conditions

$$U(x_L,t) = f_0(t), U(x_R,t) = f_1(t), t \in [0,T]$$

where U_0, f_0 and f_1 are smooth functions; $\Omega = [x_L, x_R]$, $x_L, x_R \in \mathbb{R}, 0 < T < \infty$. In Equation (1), if $F = U_x + UU_x$, then the Rosenau equation is obtained in dynamics of dense discrete systems (Rosenau, 1988). Theoretical studies on the existence and uniqueness of the solution of the Rosenau equation are carried out by Park (1993). Omrani *et al*. (2008) obtained numerical solutions by three-level finite difference. Atouani & Omrani (2015) obtained the numerical solutions by high-order FEMs. These schemes are conservative and unconditionally stable. Chung & Ha (1994) presented a study on error estimates of Galerkin FEM approximation for Rosenau equation. When $F = U_x + UU_x - U_{xx}$ is taken in Equation (1), it is known as Rosenau-Burger equation. Some numerical solutions of the equation using finite difference methods are as follows: Hu *et al*. (2008) used Crank-Nicolson, Pan & Zhang (2012a) applied linear implicit, and Janwised *et al*. (2014) utilized modified three-level average. Piao *et al*. (2016) obtained the numerical solutions by quadratic B-spline Galerkin method. Zürnacı & Seydaoğlu (2019) presented convergence analysis of operator splitting methods to the equation. In Equation (1), if $F = U_x + UU_x + U_{xxx}$, then it is called the Rosenau-KdV equation. Hu *et al*. (2013) obtained the approximate solution of the equation using the second-order conservative finite difference scheme. Uçar *et al*. (2017) obtained numerical solutions of the equation using Galerkin cubic B-spline FEM. Kutluay *et al*. (2019) obtained numerical solutions of the equation by time splitting techniques. If $F = U_x + UU_x + U_{xxx}$ is taken in Equation (1), then it is called the Rosenau-RLW equation. Zuo *et al*. (2010) applied the Crank-Nicolson finite difference scheme, Pan & Zhang (2012b) used three-level and conservative linear implicit finite difference scheme, and Atouani & Omrani (2013) proposed semidiscrete and fully discrete Galerkin methods. Yağmurlu *et al*. (2017) obtained the approximate solution of the equation by Galerkin cubic B-spline FEM. In Equation (1), if $F = U_x + UU_x + U_{xxx} + U_{xxt}$ is taken, then the Rosenau-KdV-RLW equation is obtained for modelling dispersive shallow water waves (Razborova *et al*., 2014). Wongsaijai & Poochinapan (2014) utilized implicit finite difference method, Ak & Karakoç (2016) proposed quintic B-spline collocation method, Foroutan & Ebadian (2018) used fully discrete Chebyshev pseudo-spectral scheme, Ghiloufi & Omrani (2018) applied three-level linearized compact difference scheme, Wang & Dai (2018) obtained three level linear implicit conservative finite difference scheme, Karakoç *et al*. (2018) proposed septic B-spline collocation method, and Özer (2018;2019) obtained the numerical solution using cubic and quintic B-spline collocation methods.

In this study, the numerical solutions of Rosenau-KdV-RLW equation

$$\begin{aligned} &U_t + aU_x + b\left(U^p\right)_x - cU_{xxt} + dU_{xxx} \\ &+eU_{xxxxt} = 0,\ (x,t) \in [x_L, x_R] \times [0,T] \end{aligned} \tag{2}$$

with the initial condition

$$U(x,0) = U_0(x),\ x \in [x_L, x_R] \tag{3}$$

and the boundary conditions

$$\left.\begin{aligned} U(x_L,t) = U(x_R,t) = 0, \\ U_x(x_L,t) = U_x(x_R,t) = 0 \end{aligned}\right\},\ t \in [0,T] \tag{4}$$

are obtained. U is the wave profile and U_t is linear evolution term, U_x is advection term, U_{xxx} is dispersion term, U_{xxt} and U_{xxxxt} are dissipative terms. a, b, c, d, e are real numbers, $c > 0$, $e > 0$, p is an integer greater than 1 (Ghiloufi & Omrani, 2018). To solve Rosenau-KdV-RLW equation, the two efficient numerical schemes based on B-spline finite element method (FEM) and time splitting methods are presented in the present article. In the literature, among others, the first method is used for solving mRLW equation by cubic B-spline Galerkin FEM (Karakoc *et al*., 2015). The second method is used for the solution of Burgers' equation (Sari *et al*., 2019).

The outline of the present study is as follows. In Section 2, the cubic B-spline Galerkin FEM and its stability analysis are given. In Section 3, Strang splitting cubic B-spline Galerkin FEM and its stability analysis are presented. In Section 4, a numerical example is used to test the methods, and the numerical results are given in tables and graphics. And finally in Section 5, a brief conclusion is given.

2. Scheme I: Cubic B-spline Galerkin FEM

Now, approximate solution of Rosenau-KdV-RLW equation is obtained using cubic B-spline Galerkin FEM. Rosenau-KdV-RLW equation given by Equation (2) is multiplied by weight function $W(x)$ and integrated from x_L to x_R

$$\begin{aligned} &\int_{x_L}^{x_R} W\left(U_t + aU_x + b\left(U^p\right)_x\right. \\ &\left.-cU_{xxt} + dU_{xxx} + eU_{xxxxt}\right) dx = 0. \end{aligned} \tag{5}$$

When $Z = U^{p-1}$ is taken and partial integration is applied to the fourth, fifth, and sixth terms in Equation (5), the weak form

$$\begin{aligned} &\int_{x_L}^{x_R} (WU_t + aWU_x + bpZWU_x \\ &+cW_xU_{xt} - dW_xU_{xx} + eW_{xx}U_{xxt})\, dx = \\ &\left[cWU_{xt} - dWU_{xx} - eWU_{xxxt} + eW_xU_{xxt}\right]\Big|_{x_L}^{x_R} \end{aligned}$$

is obtained. Since this equation is valid on $[x_L, x_R]$, it is applied to the typical element $e = [x_m, x_{m+1}] \subset [x_L, x_R]$ and the local transformation $\xi = x - x_m, 0 \leq \xi \leq h$ is applied, and the equation is obtained

$$\begin{aligned} &\int_0^h (WU_t + aWU_\xi + bpZWU_\xi \\ &+cW_\xi U_{\xi t} - dW_\xi U_{\xi\xi} + \\ &eW_{\xi\xi}U_{\xi\xi t})\, d\xi = [cWU_{\xi t} - dWU_{\xi\xi} \\ &-eWU_{\xi\xi\xi t} + eW_\xi U_{\xi\xi t}]\Big|_0^h . \end{aligned} \tag{6}$$

Let the approximate function corresponding to the analytical solution U of Equation (2) be U_N. Taking δ_j as the time-dependent parameter, U_N is written as linear combinations of ϕ_j cubic B-spline base functions in the literature

$$U_N(x,t) = \sum_{j=-1}^{N+1} \delta_j(t)\, \phi_j(x).$$

Since the non-zero B-spline functions on e are ϕ_{m-1}, ϕ_m, ϕ_{m+1} and ϕ_{m+2} by applying the local coordinate transformation, the approximate function on $[0,h]$ is written in terms of ξ as follows:

$$U_N(\xi,t) = \sum_{j=m-1}^{m+2} \delta_j^e(t)\, \phi_j(\xi).$$

W is taken with the same basis functions in Galerkin method. If we write U_N and cubic B-spline functions in places of U and W in Equation (6) respectively, we obtain

$$\sum_{j=m-1}^{m+2}\left\{\left(\int_0^h \phi_i\phi_j d\xi\right)\frac{\partial\delta_j^e}{\partial t}+a\left(\int_0^h \phi_i\phi_j^{'} d\xi\right)\delta_j^e\right.$$
$$+bpZ\left(\int_0^h \phi_i\phi_j^{'} d\xi\right)\delta_j^e+c\left(\int_0^h \phi_i^{'}\phi_j^{'} d\xi\right)\frac{\partial\delta_j^e}{\partial t}$$
$$\left.-d\left(\int_0^h \phi_i^{'}\phi_j^{''} d\xi\right)\delta_j^e+e\left(\int_0^h \phi_i^{''}\phi_j^{''} d\xi\right)\frac{\partial\delta_j^e}{\partial t}\right\}$$
$$=\sum_{j=m-1}^{m+2}\left[c\left(\phi_i\phi_j^{'}\right)\frac{\partial\delta_j^e}{\partial t}-d\left(\phi_i^{'}\phi_j^{''}\right)\delta_j^e\right.$$
$$\left.\left.-e\left(\phi_i\phi_j^{'''}\right)\frac{\partial\delta_j^e}{\partial t}+e\left(\phi_i^{'}\phi_j^{''}\right)\frac{\partial\delta_j^e}{\partial t}\right]\right|_0^h. \tag{7}$$

For $i,j=m-1,\ m,\ m+1,\ m+2$ the 4×4 type matrices A^e, B^e, C^e, D^e, E^e, $\tilde{B}^e$, F^e, G^e, H^e and K^e on e are calculated where

$$A_{ij}^e=\int_0^h \phi_i\phi_j d\xi,\quad B_{ij}^e=\int_0^h \phi_i\phi_j^{'} d\xi,$$

$$C_{ij}^e=\int_0^h \phi_i^{'}\phi_j^{'} d\xi,\ D_{ij}^e=\int_0^h \phi_i^{'}\phi_j^{''} d\xi,$$

$$E_{ij}^e=\int_0^h \phi_i^{''}\phi_j^{''} d\xi,\ \widetilde{B}_{ij}^e=Z_m\int_0^h \phi_i\phi_j^{'} d\xi,$$

$$F_{ij}^e=\phi_i\phi_j^{'}\Big|_0^h,\ G_{ij}^e=\phi_i\phi_j^{''}\Big|_0^h,$$

$$H_{ij}^e=\phi_i\phi_j^{'''}\Big|_0^h,\ K_{ij}^e=\phi_i^{'}\phi_j^{''}\Big|_0^h.$$

Thus, when $\delta^e=\left(\delta_{m-1}^e,\delta_m^e,\delta_{m+1}^e,\delta_{m+1}^e\right)^T$ is taken, Equation (7) is arranged as follows:

$$\left(A^e+cC^e+eE^e-cF^e+eH^e-eK^e\right)\frac{\partial\delta^e}{\partial t}$$
$$+\left(aB^e+bp\widetilde{B}^e-dD^e+dG^e\right)\delta^e=0.$$

Using this element-wise equation for e, the global equation is obtained as

$$\begin{aligned}&(A+cC+eE-cF+eH-eK)\frac{\partial\delta}{\partial t}\\&+\left(aB+bp\widetilde{B}-dD+dG\right)\delta=0.\end{aligned} \tag{8}$$

The unknowns in Equation (8) are of the form $\delta=(\delta_{-1},\delta_0,...,\delta_N,\delta_{N+1})^T$ and $N+3$ dimensional. The matrices $A, B, \widetilde{B}, C, D, E, F, G, H, K$ are $N+3$ dimensional square seventh band matrices. The generalized rows of those matrices are

$$A=\frac{h}{140}\left(1,120,1191,2416,1191,120,1\right),$$

$$B=\frac{1}{20}\left(-1,-56,-245,0,245,56,1\right),$$

$$C=\frac{1}{10h}\left(-3,-72,-45,240,-45,-72,-3\right),$$

$$D=\frac{3}{2h^2}\left(1,8,-19,0,19,-8,-1\right),$$

$$E=\frac{6}{h^3}\left(1,0,-9,16,-9,0,1\right),$$

$$\begin{aligned}\widetilde{B}=\tfrac{1}{20}&\left(-Z_1,-18Z_1-38Z_2,9Z_1-183Z_2-71Z_3,\right.\\&10Z_1+150Z_2-150Z_3-10Z_4,\\&\left.71Z_2+183Z_3-9Z_4,38Z_3+18Z_4,Z_4\right),\end{aligned}$$

$$F=\frac{3}{h}\left(0,0,0,0,0,0,0\right),$$

$$G=\frac{6}{h^2}\left(0,0,0,0,0,0,0\right),$$

$$H=\frac{6}{h^3}\left(-1,0,9,-16,9,0,-1\right),$$

$$K=\frac{18}{h^3}\left(0,0,0,0,0,0,0\right).$$

In this study, since $Z=U^{p-1}$ is taken, $Z_m=\left[\left(U_m+U_{m+1}\right)/2\right]^{p-1}$ is calculated. After eliminating the unknowns δ_{-1} and δ_{N+1} and using $\mathbf{A}=A+cC+eE-cF+eH-eK$, $\mathbf{B}(\delta)=aB+bp\widetilde{B}-dD+dG$ and $\mathbf{L}=-\mathbf{A}^{-1}\mathbf{B}(\delta)$ the initial values are obtained in the following matrix form:

$$\frac{\partial\delta}{\partial t}=\mathbf{L}(\delta)\,\delta,\quad \delta(0)=\delta^0,\quad t\in[0,T]. \tag{9}$$

Matrix $\mathbf{L}$ is $N+1$ dimensional square matrix and $\delta=(\delta_0,...,\delta_N)^T$ having a dimension of $N+1$. The integration of the IVP over time domain is obtained by RK4 method (Jain, 1984), and the numerical solution of Rosenau-KdV-RLW equation for $\forall t\in[0,T]$ is obtained. Additionally, the following inner iteration

$$\delta_{new}^{n+1}=\delta^n+\frac{\left(\delta^{n+1}-\delta^n\right)}{2} \tag{10}$$

is applied 3-5 times in each time step to improve the nonlinear term. Since the parameters at time steps $t_0, t_1, ..., t_{M-1}, t_M$ are $\delta^0, \delta^1, ..., \delta^{M-1}, \delta^M$, we need to find the parameter δ^0 to find the parameters at the next time steps.

Using the initial conditions in Equation (3), the parameters $\delta^0 = \left(\delta_{-1}^0, \delta_0^0, ..., \delta_N^0, \delta_{N+1}^0\right)^T$ are found by solving the following system of algebraic equations:

$$\begin{aligned} &U_0''(x_0, t) = U_0''(x_0), \\ &U_0(x_m, t) = U_0(x_m), \quad m = 0(1)N \\ &U_0''(x_N, t) = U_0''(x_N). \end{aligned} \tag{11}$$

2.1 Stability analysis of scheme I

In this section, the discretization of the initial boundary value problem the Equations (2)-(4) according to the position is obtained after the cubic B-spline Galerkin FEM is used. The stability of the obtained numerical solution given by the Equation (9) is investigated

$$\frac{\partial \mathbf{x}}{\partial t} = \widehat{\mathbf{L}}\mathbf{x}, \quad \mathbf{x}(0) = \mathbf{x}_0, \quad t \in [0, T].$$

For the system of linear differential equations in the form of the matrix $\widehat{\mathbf{L}}$ with eigenvalue of $\lambda_{\widehat{\mathbf{L}}}$ the stability function of the RK4 method $R(z) = 1 + z + z^2/2 + z^3/6 + z^4/24$ and the stability region are a set of $S = \left\{z \in \mathbb{C} : |R(z)| \leq 1, z = \lambda_{\widehat{\mathbf{L}}} k\right\}$ (Jain, 1984). Accordingly, for the stability of the proposed numerical solution, if the non-linear term in the matrix $\mathbf{B}(\delta)$ in the matrix $\mathbf{L}$ is linearized as $Z = \max\left(U^{p-1}\right)$, then the matrix is represented by $\widehat{\mathbf{L}}$, $\lambda_i, i = 1(1)N+1$ is enough to show $k\lambda_i \in S$. In this study, the eigenvalues of the matrix $\widehat{\mathbf{L}}$ for the values of $N =$ 560,1120, 2240 and 4480 are calculated and $k \leq 0.34$ for $N = 560$, $k \leq 0.17$ for $N = 1120$, $k \leq 0.09$ for $N = 2240$ and $k \leq 0.04$ for $N = 4480$, and all eigenvalues (except one) obtained are found in S. For values of $N =$ 560, 1120, 2240, and 4480, the graphs showing that the eigenvalues of the matrix $\widehat{\mathbf{L}}$ remain in the region S by taking $k = 0.25$, $k = 0.125$, $k = 0.0625$, and $k = 0.03125$, respectively, are given in Figures 1-2. It is seen from Figures 1-2 that as the number of nodes N grows, the eigenvalue outside the stability region approaches the stability region.

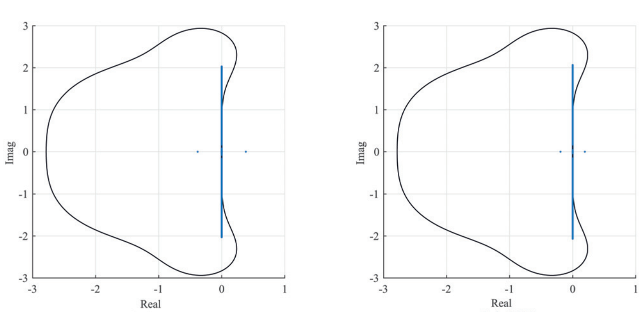

Fig. 1. Stability region for *h*=*k*=0.25 (left) and *h*=*k*=0.125 (right) (black line: RK4, blue line: Scheme I).

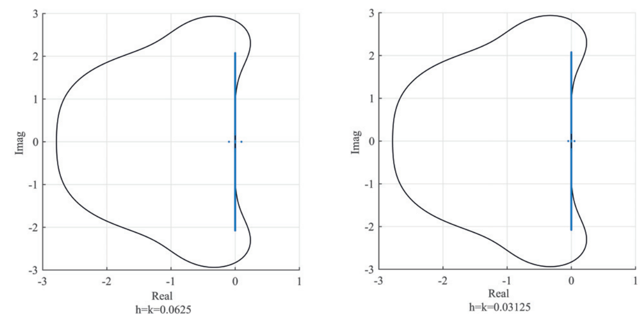

Fig. 2. Stability region for *h*=*k*=0.0625 (left) and *h*=*k*=0.03125 (right) (black line: RK4, blue line: Scheme I).

3. Scheme II: Cubic B-spline Strang Splitting Galerkin FEM

In this section, after applying the Strang splitting technique to the initial-boundary value problem given by Equations (2)-(4), the numerical solution is obtained by cubic B-spline Galerkin FEM. For this, the Rosenau-KdV-RLW equation given by Equation (2) is divided into two subequations, the first linear and the second nonlinear:

$$U_t - cU_{xxt} + eU_{xxxxt} + aU_x + dU_{xxx} = 0, \tag{12}$$

$$U_t - cU_{xxt} + eU_{xxxxt} + b\left(U^p\right)_x = 0. \tag{13}$$

To avoid any confusion, in Equation (12) in place of the variable U the variable u is written and the first equation has become

$$\begin{aligned} &u_t - cu_{xxt} + eu_{xxxxt} + au_x + du_{xxx} = 0, \\ &u(x, t_n) = U(x, t_n), t \in \left[t_n, t_{n+\frac{1}{2}}\right] \end{aligned} \tag{14}$$

Then, in Equation (13) in place of the variable U the new variable v is written and the second problem has become

$$\begin{aligned} &v_t - cv_{xxt} + ev_{xxxxt} + bpv^{p-1}v_x = 0, \\ &v(x, t_n) = u\left(x, t_{n+\frac{1}{2}}\right), t \in [t_n, t_{n+1}] \end{aligned} \tag{15}$$

and finally in Equation (12) in place of the variable U the new variable y is written and the third problem has become

$$\begin{aligned} &y_t - cy_{xxt} + ey_{xxxxt} + ay_x + dy_{xxx} = 0, \\ &y\left(x, t_{n+\frac{1}{2}}\right) = v(x, t_{n+1}), t \in \left[t_{n+\frac{1}{2}}, t_{n+1}\right]. \end{aligned} \tag{16}$$

Here, $t_{n+\frac{1}{2}} = \left(n + \frac{1}{2}\right)k$ and $u(x, t_0) = U(x, t_0) = U_0(x)$. For the initial value problems given by Equations (14), (15), and (16), the boundary conditions given by Equation (4) are used. In a similar way used in Section 2, Equations (14), (15), and (16) are multiplied by the weight function

W and integrated from x_L to x_R. Taking $Z = v^{p-1}$ and applying the partial integration, the weak forms are obtained. Let the approximate function corresponding to the analytical solution $u(x,t)$ of Equation (14) be $U_N(x,t)$, analytical solution $v(x,t)$ of Equation (15) be $V_N(x,t)$, and analytical solution $y(x,t)$ of Equation (16) be $Y_N(x,t)$. Taking the parameters δ_j, σ_j and γ_j as the time-dependent parameters, those approximations are written as follows:

$$U_N(x,t) = \sum_{j=-1}^{N+1} \delta_j(t)\,\phi_j(x),$$

$$V_N(x,t) = \sum_{j=-1}^{N+1} \sigma_j(t)\,\phi_j(x),$$

$$Y_N(x,t) = \sum_{j=-1}^{N+1} \gamma_j(t)\,\phi_j(x)$$

as linear combinations of cubic B-spline functions. Since the non-zero B-spline functions on e are ϕ_{m-1}, ϕ_m, ϕ_{m+1} and ϕ_{m+2} by applying the local coordinate transformation, the approximate functions on $[0,h]$ are written as follows in terms of ξ

$$U_N(\xi,t) = \sum_{j=m-1}^{m+2} \delta_j^e(t)\,\phi_j(\xi), \tag{17}$$

$$V_N(\xi,t) = \sum_{j=m-1}^{m+2} \sigma_j^e(t)\,\phi_j(\xi), \tag{18}$$

$$Y_N(\xi,t) = \sum_{j=m-1}^{m+2} \gamma_j^e(t)\,\phi_j(\xi). \tag{19}$$

When the local coordinate transformation is applied by writing the weak forms on a typical element e, the following equations are obtained:

$$\begin{aligned}\int_0^h &(Wu_t + aWu_\xi + cW_\xi u_{\xi t} - dW_\xi u_{\xi\xi}\\ &+eW_{\xi\xi}u_{\xi\xi t})\,d\xi = [cWu_{\xi t} - dWu_{\xi\xi}\\ &\quad -eWu_{\xi\xi\xi t} + eW_\xi u_{\xi\xi t}]|_0^h,\end{aligned} \tag{20}$$

$$\begin{aligned}\int_0^h &(Wv_t + bpZv_\xi + cW_\xi v_{\xi t}\\ &+eW_{\xi\xi}v_{\xi\xi t})\,d\xi = [cWv_{\xi t}\\ &-eWv_{\xi\xi\xi t} + eW_\xi v_{\xi\xi t}]|_0^h,\end{aligned} \tag{21}$$

$$\begin{aligned}\int_0^h &(Wy_t + aWy_\xi + cW_\xi y_{\xi t} - dW_\xi y_{\xi\xi}\\ &+eW_{\xi\xi}y_{\xi\xi t})\,d\xi = [cWy_{\xi t} - dWy_{\xi\xi}\\ &\quad = -eWy_{\xi\xi\xi t} + eW_\xi y_{\xi\xi t}]|_0^h.\end{aligned} \tag{22}$$

In Equations (20)-(22), in places of u, v and y their corresponding approximations U_N, V_N and Y_N in Equations (17)-(19) are written, and cubic B-spline functions are written in place of W, and required arrangements are made. Then, when $\delta^e = \left(\delta_{m-1}^e, \delta_m^e, \delta_{m+1}^e, \delta_{m+1}^e\right)^T$, $\sigma^e = \left(\sigma_{m-1}^e, \sigma_m^e, \sigma_{m+1}^e, \sigma_{m+1}^e\right)^T$ and $\gamma^e = \left(\gamma_{m-1}^e, \gamma_m^e, \gamma_{m+1}^e, \gamma_{m+1}^e\right)^T$ are taken, the equations are written as follows:

$$\begin{gathered}(A^e + cC^e + eE^e - cF^e + eH^e - eK^e)\,\tfrac{\partial\delta^e}{\partial t}\\ +(aB^e - dD^e + dG^e)\,\delta^e = 0,\end{gathered}$$

$$\begin{gathered}(A^e + cC^e + eE^e - cF^e + eH^e - eK^e)\,\tfrac{\partial\sigma^e}{\partial t}\\ +bp\widetilde{B}^e\sigma^e = 0,\end{gathered}$$

$$\begin{gathered}(A^e + cC^e + eE^e - cF^e + eH^e - eK^e)\,\tfrac{\partial\gamma^e}{\partial t}\\ +(aB^e - dD^e + dG^e)\,\gamma^e = 0.\end{gathered}$$

Using these local equations on e, the global equations on $[x_L, x_R]$ are written as the following system of differential equations:

$$\begin{aligned}&(A + cC + eE - cF + eH - eK)\,\tfrac{\partial\delta}{\partial t}\\ &\quad +(aB - dD + dG)\,\delta = 0,\end{aligned} \tag{23}$$

$$\begin{aligned}&(A + cC + eE - cF + eH - eK)\,\tfrac{\partial\sigma}{\partial t}\\ &\quad +bp\widetilde{B}\sigma = 0,\end{aligned} \tag{24}$$

$$\begin{aligned}&(A + cC + eE - cF + eH - eK)\,\tfrac{\partial\gamma}{\partial t}\\ &\quad +(aB - dD + dG)\,\gamma = 0.\end{aligned} \tag{25}$$

The unknowns in the system of ODEs given by Equations (23)-(25) are $\delta = (\delta_{-1}, \delta_0, ..., \delta_N, \delta_{N+1})^T$, $\sigma = (\sigma_{-1}, \sigma_0, ..., \sigma_N, \sigma_{N+1})^T$, $\gamma = (\gamma_{-1}, \gamma_0, ..., \gamma_N, \gamma_{N+1})^T$ and $N+3$ dimensional and $\mathbf{A} = A + cC + eE - cF + eH - eK$, $\mathbf{B_1} = aB - dD + dG$, $\mathbf{B}_2 = bp\widetilde{B}$ also $\mathbf{A}$, $\mathbf{B_1}$ and $\mathbf{B}_2$ are $N+3$ dimensional square matrices. The matrices $A, B, \widetilde{B}, C, D, E, F, G, H$ and K are seventh band matrices, and their generalized rows are the same as given in Section 2. Since the boundary conditions are not applied, solving these systems, we have not solved the IVP given by Equations (2)-(4). By applying the boundary conditions given by Equation (4), the parameters δ_{-1}, δ_{N+1}, σ_{-1}, σ_{N+1}, γ_{-1} and γ_{N+1} are eliminated from the corresponding equations. After applying the boundary conditions, the unknowns are $\delta = (\delta_0, \delta_1, ..., \delta_N)^T$, $\sigma = (\sigma_0, \sigma_1, ..., \sigma_N)^T$, $\gamma = (\gamma_0, \gamma_1, ..., \gamma_N)^T$ and their dimension is $N+1$. When the matrices $\mathbf{A}$, $\mathbf{B_1}$ and $\mathbf{B}_2$ are arranged as being compatible with $N+1$ dimensional parameters, $N+1$ dimensional square matrices are restructured. Under these conditions, taking $\mathbf{L_1} = -\mathbf{A}^{-1}\mathbf{B_1}$, $\mathbf{L_2} = -\mathbf{A}^{-1}\mathbf{B_2}(\sigma)$ the ODEs given by Equations (23)-(25) are written as follows:

$$\frac{\partial \delta}{\partial t} = \mathbf{L_1}\delta,\, \delta\left(t_n\right) = \delta^n,\, t \in \left[t_n, t_{n+\frac{1}{2}}\right], \tag{26}$$

$$\frac{\partial \sigma}{\partial t} = \mathbf{L_2}(\sigma)\,\sigma,\, \sigma\left(t_n\right) = \delta^{n+\frac{1}{2}},\, t \in \left[t_n, t_{n+1}\right], \tag{27}$$

$$\frac{\partial \gamma}{\partial t} = \mathbf{L_1}\gamma,\, \gamma\left(t_n\right) = \sigma^{n+1},\, t \in \left[t_{n+\frac{1}{2}}, t_{n+1}\right]. \tag{28}$$

Then, these ODE systems are solved by RK4 method. The γ^{n+1} parameters obtained from the solution of the ODEs system given by Equation (28) are written in their places in Equation (26) containing the parameters in the following time steps by replacing δ^n. To calculate $\delta^{\frac{1}{2}}$ the initial parameter δ^0 must be known. From the solution of the equation system given by Equation (11) as in Section 2, the initial parameter δ^0 is obtained. Approximate solutions are made better by applying 3-5 times the inner iteration given in Equation (10) at each time step to the nonlinear term in the system of equations given by Equation (27).

3.1 Stability analysis of scheme II

In this section, after applying the Strang splitting technique to the initial-boundary value problem given by Equations (2)-(4), its discretization with respect to spatial

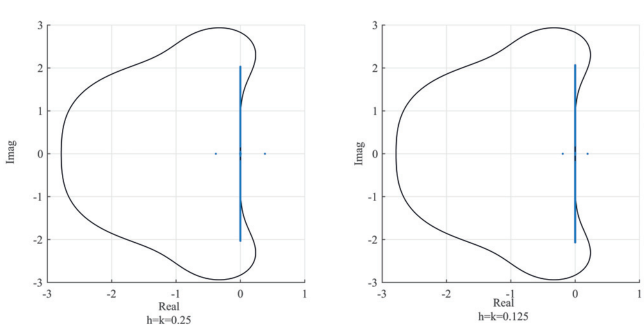

Fig. 3. Stability region for *h*=*k*=0.25 (left) and *h*=*k*=0.125 (right)(black line: RK4, blue line: Scheme II).

variable is made with cubic B-spline Galerkin FEM, and the obtained equations are given by Equations (26)-(28), and the numerical solutions of those ODE systems are obtained by the application of RK4 method, and the stability of those equations is investigated. After linearizing the nonlinear term in the matrix $\mathbf{L_2}\left(\sigma\right)$ as $Z = \max\left(v^{p-1}\right)$

$$\widehat{\mathbf{L}} = \begin{bmatrix} \mathbf{L_1} & \mathbf{O} & \mathbf{O} \\ \mathbf{O} & \mathbf{L_2} & \mathbf{O} \\ \mathbf{O} & \mathbf{O} & \mathbf{L_1} \end{bmatrix}$$

it is enough to show that $k\lambda_i \in S$ for $\lambda_i, i=1(1)N+1$ where λ_i are the eigenvalues of the square matrix $\widehat{\mathbf{L}}$ of type $3N+3$ (Jain, 1984). Here, the matrix $\mathbf{O}$ is the $N+1$ dimensional square zero matrix. In this study, the eigenvalues of the matrix $\widehat{\mathbf{L}}$ for the values of $N=560, 1120, 2240$ and 4480 have been calculated and $k \leq 0.34$ for $N=560$, $k \leq 0.17$ for $N=1120$, $k \leq 0.09$ for $N=2240$ and $k \leq 0.04$ for $N=4480$, and all the eigenvalues (except one) obtained have been found in the S region. Then, for values of N = 560, 1120, 2240 and 4480, the graphs showing that the eigenvalues of the matrix $\widehat{\mathbf{L}}$ remain in the region S are given. Taking $k=0.25$, 0.125, 0.0625 and 0.03125, the graphs showing that they lie inside the region S are illustrated in Figures 3-4, respectively. Thus, the larger the number N, the smaller the time step k required to satisfy the stability condition of the eigenvalues of the matrix $\widehat{\mathbf{L}}$. From Figures 3-4, as the number of nodes N grows, it is seen that the eigenvalue outside the stability region approaches the stability region.

4. Numerical results and comparisons

In this section, the numerical results obtained by applying the methods are proposed in Sections 2-3 to an example for Rosenau-KdV-RLWequation. To show the effectiveness

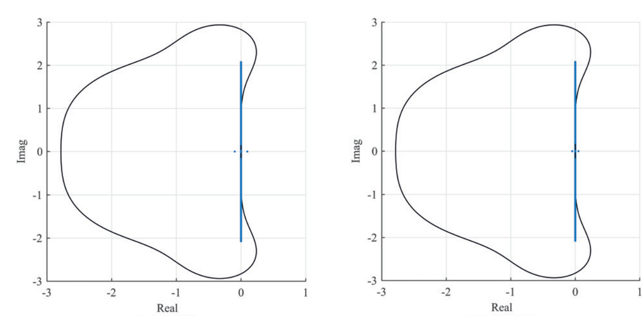

Fig. 4. Stability region for *h*=*k*=0.0625 (left) and *h*=*k*=0.03125 (right) (black line: RK4, blue line: Scheme II).

and reliability of the methods, fundamental conservative properties defined as

$$Q(t) = \int_{x_L}^{x_R} U(x,t)dx \tag{29}$$

$$E(t)=\int_{x_L}^{x_R}\left[U^2(x,t)+cU_x^2(x,t)+U_{xx}^2(x,t)\right]dx \quad (30)$$

for mass and energy conservation constants,

$$L_2=\sqrt{h\sum_{i=1}^{N}\left|U(x,t)-U_N(x,t)\right|^2},$$

$$L_\infty=\max_{1\le i\le N}\left|U(x,t)-U_N(x,t)\right|$$

the error norms as defined above and L being any one of the above error norms the rate of convergence defined as below,

$$Rate=\log_2\left(\frac{L(2h,2t)}{L(h,t)}\right)$$

are calculated. All numerical calculations were obtained using Matlab2015a program on 4G RAM, 2.20 GHz computer.

Example: The analytical solution of the Rosenau-KdV-RLW equation given by Equation (2) for parameters $a=1$, $b=0.5$, $c=1$, $d=1$, $e=1$, $p=2$ is (Wang, 2018)

$$U(x,t)=k_1\sec h^4\left(k_2\left(x-k_3t\right)\right)$$

where

$$k_1=\frac{-5\left(25-13\sqrt{457}\right)}{456},\quad k_2=\frac{\sqrt{-13+\sqrt{457}}}{\sqrt{288}},$$

$$k_3=\frac{241+13\sqrt{457}}{266}.$$

The initial condition of the problem is obtained writing $t=0$ in the analytical solution. In Tables 1-2 for $x_L=-40$, $x_R=100$ at the time $T=30$ the error norms L_2 and L_∞ obtained by cubic B-spline Galerkin and cubic B-spline Strang Galerkin methods are compared with those of the numerical solutions given in the literature. As seen from Tables 1-2, the errors of the numerical solutions obtained by the presented methods are smaller than those of the compared methods.

By taking $x_L=-40$, $x_R=100$ at the time $T=30$, the convergence rates for the error norms L_2 and L_∞ obtained for cubic B-spline Galerkin and cubic B-spline Strang Galerkin FEMs are calculated and given in Tables 3-4, respectively. The convergence rates of the proposed methods are compared with the convergence rates of the studies (Wang, 2018) and (Özer, 2019). Although the error norms L_2 and L_∞ of the methods are smaller, it is seen that there is a fluctuation in convergence rates. For values of $T=0$, $x_L=-40$, $x_R=160$, the mass and energy conservation constants are calculated as $Q=21.67925844$ and $E=43.71719866$ from Equations (29)-(30). For values of $x_L=-40$, $x_R=160$, $k=h=0.25$ at times $T=15,\ 30,\ 45,\ 60$, the mass and energy conservation constants are calculated using the proposed methods and compared with the results of Wongsaijai (2014) and Özer (2019) in Tables 5-6. According to the results, it is seen that the fundamental conservation properties of the Rosenau-KdV-RLW equation on the interval $[0,\ 60]$ have slightly deteriorated with the proposed numerical schemes. Then, in Tables 7-8 for values of $h=0.25$ and $k=0.125$, 0.0625, 0.03125 at times $T=15,30,45,60$, the mass and energy conservation constants are calculated by the recommended methods. It is seen from Tables 7-8 that, to maintain the mass and energy conservation constants in the future, a small selection of the parameter k is required. In Figures 5-6 over the range of $[-40,\ 100]$, the graphs of the analytical solutions at the time T = 0,10,20,30 with $h=k=0.25$ for the cubic B-spline Galerkin and cubic B-spline Strang Galerkin FEMs obtained from numerical solution and the graphs of absolute errors at times $T=$ 10,20,30 are given. The height of the wave in the analytical solution is $U(0,0)=2.7731$, and the height of the wave by the proposed methods is $U_G(19.5,\ 10)=2.7698$, $U_G(39,\ 20)=2.7684$, $U_G(58.5,\ 30)=2.7670$, $U_{SG}(19.5,\ 10)=2.7714$, $U_{SG}(39,\ 20)=2.7705$,

Table 1. A comparison of numerical results using the error norm L_2 for various $h=k$ and $x\in[-40,\ 100]$ at time $T=30$.

$h=k$	Scheme I	Scheme II	Wongsaijai (2014) $\theta=-1$	Wang (2018)	Özer (2018) Scheme II	Özer (2019) Strang
0.25	$1.58026E-2$	$8.34849E-3$	$5.56190E-1$	$1.86617E-0$	$2.37668E-1$	$9.58702E-2$
0.125	$7.09775E-3$	$3.94750E-3$	$1.34741E-1$	$5.18662E-1$	$6.00345E-2$	$2.41393E-2$
0.0625	$2.25510E-3$	$1.29341E-3$	$3.34447E-2$	$1.33174E-1$	$1.50476E-2$	$6.04596E-3$
0.03125	$6.24645E-4$	$3.62866E-4$	–	$3.35296E-2$	$3.76437E-3$	$1.51234E-3$

Table 2. A comparison of numerical results using the error norm L_∞ for various $h = k$ and $x \in [-40, 100]$ at time $T = 30$.

$h = k$	Scheme I	Scheme II	Wongsaijai (2014) $\theta = -1$	Wang (2018)	Özer (2018) Scheme II	Özer (2019) Strang
0.25	$6.62692E-3$	$3.69796E-3$	$2.14488E-1$	$6.99597E-1$	$9.10323E-2$	$3.70795E-2$
0.125	$2.68306E-3$	$1.44497E-3$	$5.19201E-2$	$1.97127E-1$	$2.30177E-2$	$9.33938E-3$
0.0625	$8.83886E-4$	$4.94883E-4$	$1.28858E-2$	$5.06954E-2$	$5.76980E-3$	$2.33925E-3$
0.03125	$2.47568E-4$	$1.40963E-4$	–	$1.27669E-2$	$1.44360E-3$	$5.85173E-4$

Table 3. A comparison of convergence rates for the error norm L_2 at $T = 30$.

$h = k$	Scheme I	Scheme II	Wongsaijai (2014) $\theta = -1$	Wang (2018)	Özer (2018) Scheme II	Özer (2019) Strang
0.25	3.17238	3.31169	2.21285	1.84721	1.93992	1.96108
0.125	1.15473	1.08058	2.04539	1.96149	1.98508	1.98970
0.0625	1.65417	1.60976	2.01034	1.98980	1.99625	1.99734
0.03125	1.85208	1.83367	–	–	–	1.99919

Table 4. A comparison of convergence rates for the error norm L_∞ at $T = 30$.

$h = k$	Scheme I	Scheme II	Wongsaijai (2014) $\theta = -1$	Wang (2018)	Özer (2018) Scheme II	Özer (2019) Strang
0.25	3.23655	3.32927	2.20179	1.82740	1.92951	1.95614
0.125	1.30446	1.35569	2.04653	1.95920	1.98363	1.98922
0.0625	1.60195	1.54588	2.01051	1.98945	1.99838	1.99728
0.03125	1.83604	1.81177	–	–	–	1.99911

Table 5. A comparison of mass invariants for $h = k = 0.25$, $x \in [-40, 160]$ at $T = 30$.

T	Scheme I	Scheme II	Wongsaijai (2014) $\theta = -1$	Özer (2018) Scheme II	Özer (2019) Strang
0	21.67925844	21.67925844	21.67925844	21.67925844	21.67925844
15	21.66232590	21.66833634	21.68257703	21.67922326	21.67923476
30	21.64547429	21.65744876	21.68264127	21.67919310	21.67921009
45	21.62853523	21.64656881	21.68342617	21.67891685	21.67903058
60	21.61343158	21.63629834	21.67462536	21.68069226	21.68137637

Table 6. A comparison of energy invariants for $h = k = 0.25$, $x \in [-40, 160]$.

T	Scheme I	Scheme II	Wongsaijai (2014) $\theta = -1$	Özer (2018) Scheme II	Özer (2019) Strang
0	43.70855146	43.70855146	43.70855146	43.70855146	43.70855146
15	43.65552275	43.67433910	43.72652015	43.71412237	43.71413508
30	43.60244732	43.64014854	43.72664228	43.71401660	43.71406292
45	43.54958713	43.60605430	43.72664409	43.71391006	43.71399045
60	43.49694776	43.57205751	43.72664408	43.71380341	43.71391799

Table 7. A comparison of mass and energy invariants obtained by Scheme I for $h = 0.25$, $k = 0.125$, 0.0625, 0.03125, $x \in [-40,\ 160]$.

	$k = 0.125$		$k = 0.0625$		$k = 0.03125$	
T	Q	E	Q	E	Q	E
0	21.67925844	43.70855146	21.67925844	43.70855146	21.67925844	43.70855146
15	21.67713954	43.70210063	21.67899367	43.70780173	21.67922538	43.70850659
30	21.67502087	43.69554915	21.67872766	43.70698665	21.67919111	43.70840538
45	21.67282341	43.68899932	21.67839978	43.70617076	21.67909953	43.70830351
60	21.67171697	43.68245283	21.67899351	43.70535490	21.67988777	43.70820161

Table 8. A comparison of mass and energy invariants ontained Scheme II for $h = 0.25$, $k = 0.125$, 0.0625, 0.03125, $x \in [-40,\ 160]$.

	$k = 0.125$		$k = 0.0625$		$k = 0.03125$	
T	Q	E	Q	E	Q	E
0	21.67925844	43.70855146	21.67925844	43.70855146	21.67925844	43.70855146
15	21.67789208	43.70434777	21.67908772	43.70807567	21.67923713	43.70853967
30	21.67652554	43.70008122	21.67891586	43.70754338	21.67921463	43.70847371
45	21.67511210	43.69581531	21.67869027	43.70701044	21.67913687	43.70840711
60	21.67449177	43.69155089	21.67931206	43.70647750	21.67992039	43.70834050

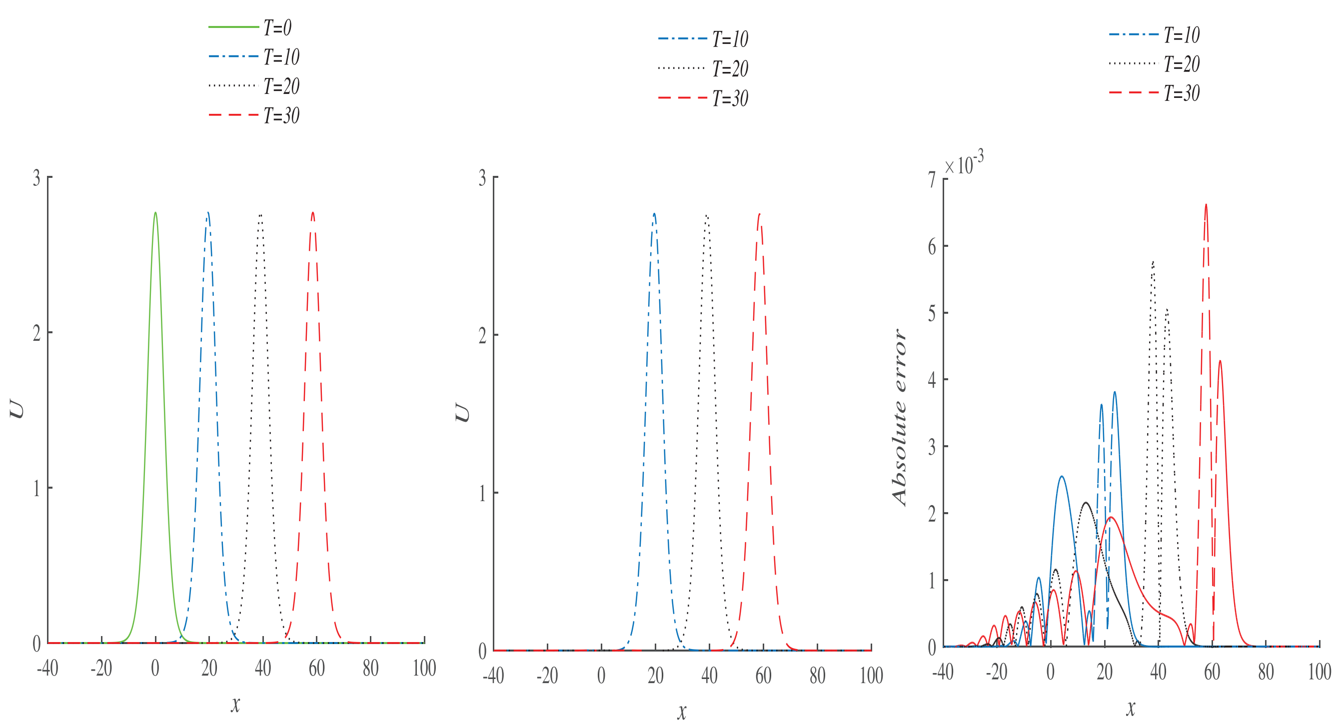

Fig. 5. Analitical solution (left), numerical solution obtained by Scheme I for $h = k = 0.25$ (middle), absolute error (right).

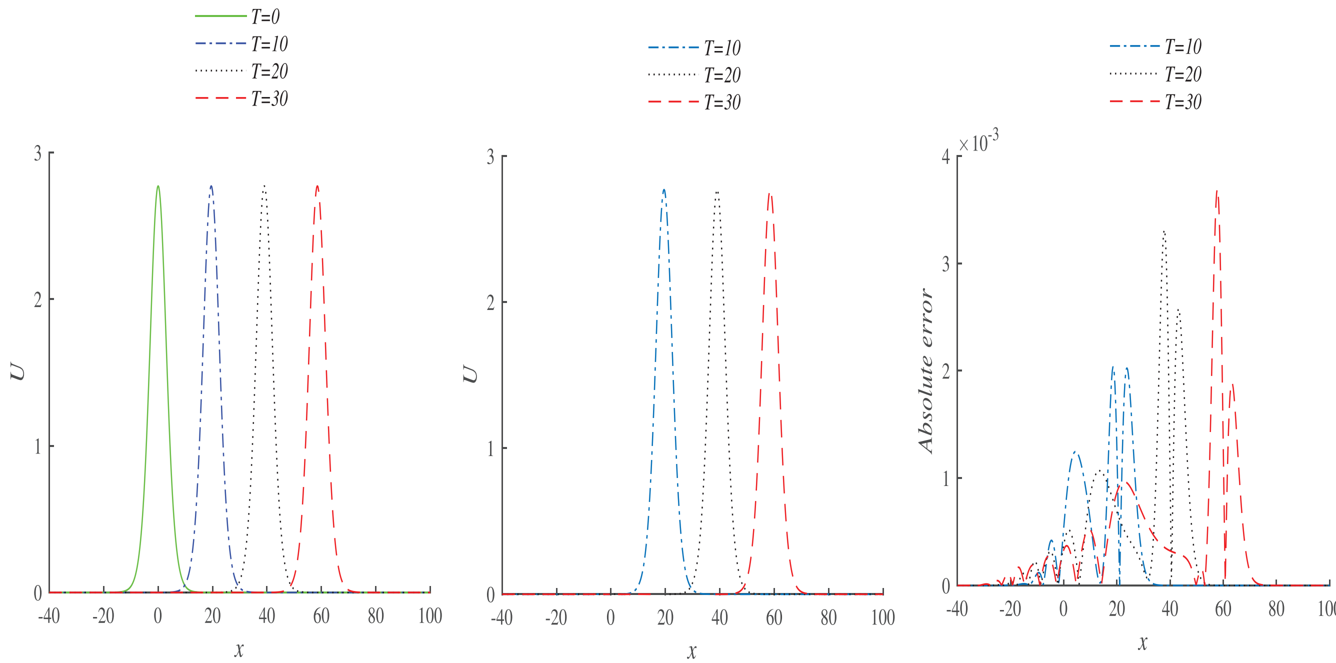

Fig. 6. Analitical solution (left), numerical solution obtained by Scheme II for $h = k = 0.25$ (middle), absolute error (right).

$U_{SG}(58.5,\ 30) = 2.7696$. Here, G and SG subscripts show the FEMs of cubic Galerkin and cubic Strang Galerkin, respectively. From Figures 5-6, it is seen that the numerical solutions and analytical solutions are compatible with each other, but as time progresses, the height of the wave decreases and thus, the absolute error increases. Additionally, the absolute error of the cubic B-spline Strang Galerkin method is less than that of the cubic B-spline method.

5. Conclusion

In this study, numerical solutions of Rosenau-KdV-RLW equation are obtained using cubic B-spline Galerkin and cubic B-spline Strang-splitting Galerkin FEMs. To show the accuracy and efficiency of the methods, those methods are applied to a test problem of which analytical solution is known. The mass and energy invariants, the error norms L_2 and L_∞ with the convergence rates are calculated. It is seen that the proposed methods yield good enough results. The illustrative test problem shows that the error norms are small enough and the conservation laws are nearly constant. In conclusion, numerical solutions of other important high-order nonlinear partial differential equations widely seen in various fields of science can be achieved easily and effectively by using the proposed methods.

References

Ak, T., Karakoc, S.B.G. & Biswas A. (2016). Numerical scheme to dispersive shallow water waves. Journal of Computational and Theoretical Nanoscience, **13**:7084-7092.

Atouani, N. & Omrani, K. (2013). Galerkin finite element method for the Rosenau-RLW equation. Computers and Mathematics with Applications, **66**:289-303.

Atouani, N. & Omrani, K. (2015). A new conservative high-order accurate difference scheme for the Rosenau equation. Applicable Analysis, **94**:2435-2455.

Chung, S.K & Ha, S.N. (1994). Finite element Galerkin solutions for the Rosenau equation. Applicable Analysis, **54**(1-2):39-56.

Foroutan, M. & Ebadian, A. (2018). Chebyshev rational approximations for the Rosenau-KdV-RLW equation on the whole line. International Journal of Analysis and Applications,**16**(1):1-15.

Ghiloufi, A. & Omrani, K. (2018). New conservative difference schemes with fourth-order accuracy for some model equation for nonlinear dispersive waves. Numerical Methods for Partial Differential Equations, **34**:451-500.

Hu, B., Xu, Y. & Hu, J. (2008). Crank-Nicolson finite difference scheme for the Rosenau-Burgers equation. Applied Mathematics and Computation, **204**(1):311-316.

Hu, J., Xu, Y. & Hu, B. (2013). Conservative linear difference scheme for Rosenau-KdV equation. Advances in Mathematical Physics, Article ID 423718. 7 pages.

Jain, M.K. (1984). Numerical solution of differential equations. Wiley Eastern, New Delhi, India.

Janwised, J., Wongsaijai, B., Mouktonglang, T. & Poochinapan, K. (2014). A Modified Three-level average linear-implicit finite difference method for the Rosenau-Burgers equation. Advances in Mathematical Physics, Article ID 734067, 11 pages.

Karakoç, S.B.G., Uçar, Y. & Yağmurlu, N.M. (2015). Numerical solutions of the MRLW equation by cubic B-spline Galerkin finite element method. Kuwait Journal of Science, **42**(2):141-159.

Karakoç, S.B.G., Gao, F. & Bhowmik, S.K. (2018). Solitons and shock waves solutions for the Rosenau-KdV-RLW equation. Journal of Science and Arts, **4**(45):1073-1088.

Kutluay, S., Karta, M. & Yağmurlu, N.M. (2019). Operator time-splitting techniques combined with quintic B-spline collocation method for the generalized Rosenau–KdV equation. Numerical Methods for Partial Differential Equations, **35**:2221-2235.

Omrani, K., Abidi, F., Achouri, T. & Khiari, N. (2008). A new conservative finite difference scheme for the Rosenau equation. Applied Mathematics and Computation, **201**:35-43.

Özer, S. (2018). An effective numerical technique for the Rosenau-KdV-RLW equation. Journal of Balikesir University Institute of Science and Technology, **20**(3):1-14.

Özer, S. (2019). Numerical solution of the Rosenau-KdV-RLW equation by operator splitting techniques based on B-spline collocation method. Numerical Methods for Partial Differential Equations, **35**:1928-1943.

Pan, X. & Zhang, L. (2012a). A new finite difference scheme for the Rosenau-Burgers equation. Applied Mathematics and Computation, **218**(17):8917-8924.

Pan, X. & Zhang, L. (2012b). On the convergence of a conservative numerical scheme for the usual Rosenau-RLW equation. Applied Mathematical Modelling, **36**:3371-3378.

Park, M.A. (1993). On the Rosenau equation in multidimensional space. Nonlinear Analysis, **21**:77-85.

Piao, G.R., Lee, J.Y. & Cai, G.X. (2016). Analysis and computational method based on quadratic B-spline FEM for the Rosenau-Burgers equation. Numerical Methods for Partial Differential Equations, **32**(3):877-895.

Prenter, P.M. (1975). Splines and variational methods. John Wiley and Sons, New York.

Razborova, P., Ahmed, B. & Biswas, A. (2014). Solitons, shock waves and conservation laws of Rosenau-KdV-RLW equation with power law nonlinearity. Applied Mathematics & Information Sciences, **8**(2):485-491.

Sari, M., Tunc, H. & Seydaoglu, M. (2019). Higher order splitting approaches in analysis of the Burgers equation. Kuwait Journal of Science, **46**(1):1-14.

Ucar, Y., Karaagac, B. & Kutluay, S. (2017). A Numerical approach to the Rosenau-KdV equation using Galerkin cubic finite element method. International Journal of Applied Mathematics and Statistics, **56**(3):83-92.

Wang, X. & Dai, W. (2018). A three-level linear implicit conservative scheme for the Rosenau-KdV-RLW equation. Journal of Computational and Applied Mathematics, **330**:295-306.

Wongsaijai, B. & Poochinapan, K. (2014). A three-level average implicit finite difference scheme to solve equation obtained by coupling the Rosenau-KdV equation and Rosenau-RLW equation. Applied Mathematics and Computation, **245**:289-304.

Yagmurlu, N.M., Karaagac, B. & Kutluay, S. (2017). Numerical solutions of Rosenau-RLW Equation using Galerkin cubic B-Spline finite element method. American Journal of Computational and Applied Mathematics, **7**(1):1-10.

Zuo, J.M., Zhang, Y.M., Zhang, T.D. & Chang, F. (2010). A new conservative difference scheme for the general Rosenau–RLW equation. Boundary Value Problems, 13. Article ID 516260.

Zürnacı, F. & Seydaoğlu, M. (2019). On the convergence of operator splitting for the Rosenau-Burgers equation. Numerical Methods for Partial Differential Equations, **35**:1363-1382.

Submitted : 12/11/2019

Revised : 01/03/2020

Accepted : 08/03/2020

DOI : 10.48129/kjs.v48i1.8610